

Selective formation 2,6-diisopropyl naphthalene over mesoporous Al-MCM-48 catalysts

T. Krithiga^a, A. Vinu^{b,*}, K. Ariga^c, B. Arabindoo^a,
M. Palanichamy^a, V. Murugesan^a

^a Department of Chemistry, Anna University, Chennai 600025, India

^b International Center for Young Scientists, National Institute for Materials Science, 1-1 Namiki, Tsukuba, Ibaraki 305-0044, Japan

^c Supermolecules Group, Advanced Materials Laboratory, National Institute for Materials Science, 1-1 Namiki, Tsukuba 305-0044, Japan

Received 21 April 2005; received in revised form 4 May 2005; accepted 5 May 2005

Available online 13 June 2005

Abstract

The protonated cubic mesoporous aluminosilicate (Al-MCM-48) molecular sieves have been synthesized hydrothermally and characterized by powder X-ray diffraction (XRD), nitrogen adsorption studies, thermogravimetric analysis (TGA) and solid-state ²⁹Si and ²⁷Al MAS NMR spectroscopy. The XRD patterns and nitrogen adsorption results reveal the cubic structural order and the mesoporous nature of the catalysts. ²⁷Al MAS NMR spectra demonstrate that most of the Al is incorporated in the framework in tetrahedral coordination. Acidity measurement by pyridine-adsorbed FT-IR spectroscopy reveals that the incorporation of Al in the framework imparts substantial Brønsted acidity, which increases with increase in metal content. Lewis acidity is probably generated by extra-framework Al species. Vapour phase isopropylation of naphthalene (NAP) with isopropyl alcohol (IPA) was carried out over H-form of Al-MCM-48 catalysts with different $n_{\text{Si}}/n_{\text{Al}}$ ratios. The feed molar ratio of 1:2:10 (NAP:IPA:CYH) and WHSV (5.36 h^{-1}) were found to be the optimized conditions for good NAP conversion with selectivity of 2,6-diisopropylnaphthalene (2,6-DIPN). The effect of 2,6/2,7-DIPN ratio was also studied for catalysts with various $n_{\text{Si}}/n_{\text{Al}}$ ratios and at different temperatures. Among the catalysts used in the present study, AlMCM-48 (25) showed a high NAP conversion and selectivity to 2,6-DIPN under the optimized reaction conditions.

© 2005 Elsevier B.V. All rights reserved.

Keywords: Mesoporous; Al-MCM-48; Cubic; Naphthalene; β, β' -Selectivity; Isopropylation

1. Introduction

Mobil Oil Research and Development reported the direct synthesis of the first broad family of mesoporous molecular sieves (M41S) using cationic surfactants to assemble silicate anions from solution [1,2]. The main difference in the synthesis of MCM-48 and MCM-41 is surfactant to silica ratio in the synthesis solution [3]. Huo et al. [4] rationalized MCM-48 synthesis by carefully selecting the surfactants that favour cubic mesophase. MCM-48 materials have been

studied less intensively than MCM-41 materials probably due to smaller synthesis regime of MCM-48. Pure silica materials do not possess enough intrinsic acidity or reactivity to be used as catalyst. Therefore, much attention has been devoted to isomorphic substitution of other elements like Al into the wall structure of these materials [5–11]. Aluminium incorporation into the mesoporous silica materials can generate both Brønsted and Lewis acidities required for acid-catalyzed reactions [8,12,13]. Al-MCM-48 materials have been exploited very little than Al-MCM-41 [14,15] because of the limited reproducible synthetic methods and sensitive synthesis parameters. The three dimensional Al-MCM-48 materials with large surface area, high pore volume and very narrow pore size distributions offer limited pore

* Corresponding author. Tel.: +81 29 851 3354x8679; fax: +81 29 860 4706.

E-mail address: vinu.ajayan@nims.go.jp (A. Vinu).

plugging problems and the particles are more readily accessible because the pore openings are not restricted in one direction. This increases the number of interactions between reactants and catalytic active sites. Thus Al-MCM-48 has greater potential for adsorption or ion exchange capacity than Al-MCM-41. In a reaction system that involves reactants with polarities, the hydrophobic/hydrophilic nature of the catalyst is important factor, which influences the catalytic performance.

In the present investigation, catalytic activity of Al-MCM-48 in the isopropylation of naphthalene (NAP) has been studied. The alkylation of NAP is an important reaction as the product 2,6-diisopropylnaphthalene (2,6-DIPN) can be used as a raw material for the production of advanced aromatic polymeric materials such as polyethylene naphthalene-2,6-dicarboxylate (PEN), films and thermotropic liquid crystalline polymers [16]. Separation of 2,6-DIPN from the rest of the isomers is difficult and hence selective production of this isomer is highly desired. Isopropylation of NAP has been reported by other researchers [17–20]. Katayama et al. [20] observed the formation of 2,6-DIPN selectively in the liquid phase alkylation of NAP with propene or propan-2-ol over H-mordenite catalyst. The process of dealumination showed better 2,6-DIPN selectivity than un-modified H-Y zeolite [21] and H-mordenite [22]. Moreover, few researchers have reported the alkylation of NAP over various metal substituted uni-dimensional mesoporous materials [23–25] and tried to obtain a higher selectivity for 2,6-DIPN. In this article, we report the results of the isopropylation of NAP over three dimensional Al-MCM-48 with different $n_{\text{Si}}/n_{\text{Al}}$ ratios. We have found that Al-MCM-48 is a promising catalyst for isopropylation of NAP. Further the physico-chemical characteristics and acidity of the catalysts are correlated with catalytic activity and selectivity. The key challenge is to obtain 2,6-DIPN with high selectivity and high 2,6/2,7-DIPN ratio.

2. Experimental

2.1. Materials and methods

Tetraethylorthosilicate (TEOS; Merck), aluminium hydroxide (Merck) and *N*-hexadecyltrimethylammonium bromide (Merck) were used as the sources for silicon, aluminium and surfactant respectively. In a typical synthesis of sodium form of Al-MCM-48, TEOS was added slowly to a solution of *N*-hexadecyltrimethylammonium bromide dissolved in distilled water. NaOH (1M) was added for the gel formation and the pH was maintained at 11.6. The gel was then stirred for 30 min at room temperature (solution I). The required amount of aluminium hydroxide in 31.2 ml water was stirred for 2 h at 80 °C (Solution II). The aluminium hydroxide solution was added slowly under constant stirring to solution I. The resulting mixture was then stirred for 1 h at room temperature. The mixture was transferred into a polypropylene bottle and kept in

air oven at 100 °C for 72 h. The solid product obtained was washed with distilled water and dried at 100 °C. The dried as-synthesized material was calcined at 550 °C for 1 h in nitrogen atmosphere followed by 6 h in air to remove the organic template. The Na form of Al-MCM-48 was converted to H form by repeated ion exchange with 1 M ammonium nitrate followed by calcination at 550 °C for 6 h in air.

2.2. Characterization

The powder X-ray diffraction patterns were recorded on a Siemens D5005 diffractometer using Cu K α ($\lambda = 0.154$ nm) radiation. The diffractograms were recorded in the 2θ range 0.8–10° with a 2θ step size of 0.01° and a step time of 10 s. Nitrogen adsorption and desorption isotherms were measured at 77 K on a Quantachrome Autosorb 1 sorption analyzer. All samples were outgassed for 3 h at 250 °C under vacuum ($P < 10^{-5}$ hPa) in the degas port of the adsorption analyzer. The specific surface area was calculated using BET method. The pore diameter of the materials was obtained from the adsorption branch of the nitrogen isotherms using the corrected form of the Kelvin equation by means of Barrett–Joyner–Halenda method.

The ^{27}Al MAS NMR spectra were recorded on an MSL 400 spectrometer equipped with a magic angle-spinning (MAS) unit. The ^{27}Al MAS NMR were recorded at a frequency of 104.22 MHz, a spinning rate of 8 KHz, a pulse length of 1.0 μs , a delay time of 0.2 s, a spectral width of 330 ppm and 150 scans. The ^{27}Al chemical shifts were reported in relation to the liquid solution of aluminium nitrate. ^{29}Si MAS NMR spectra were recorded on a BRUKER MSL 400 spectrometer using single-pulse excitation with standard 7 mm rotors. The resonance frequency was 79.49 MHz. Tetramethylsilane (TMS) was employed as the chemical shift reference. Pyridine adsorbed FT-IR spectroscopic technique was employed for acidity measurement. Finely ground catalyst sample was pressed into self-supported thin wafer. The wafer was placed on a sample holder and evacuated to 10^{-6} Torr at 500 °C for 2 h and then cooled to 100 °C before recording the spectrum of the sample prior to pyridine adsorption. Then the sample was exposed to pyridine vapours at ambient temperature for 1 h. The wafer was cooled and evacuated for 1 h. The spectra of the wafer samples were recorded in absorbance mode on a Nicolet 800 (AVATAR) FT-IR spectrometer fully controlled by OMNIC software.

2.3. Catalytic run

The catalytic experiments were carried out at atmospheric pressure using a fixed-bed glass reactor in the temperature range 250–400 °C using cyclohexane as solvent. All the reactions were carried out using about 0.5 g of the catalyst. The catalysts were pressed without binder, crushed and sieved to obtain particles with a size of 250–350 μm . The catalyst packed in the middle of the reactor was activated by flowing

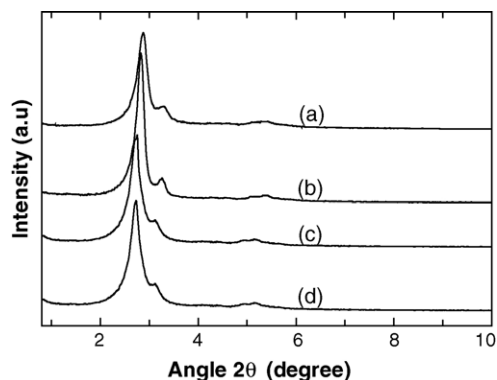


Fig. 1. XRD patterns of calcined Al-MCM-48 catalysts with different n_{Si}/n_{Al} ratios: (a) Al-MCM-48 (25); (b) Al-MCM-48 (50); (c) Al-MCM-48 (75); and (d) Al-MCM-48 (100).

air at 500 °C for 5 h inside a temperature-controlled furnace with a thermocouple placed at the centre of the catalyst bed for measuring the reaction temperature. The feed (mixture of NAP, IPA and cyclohexane) was fed into the reactor using a syringe infusion pump at predetermined flow rate. The product mixture was collected after a time interval of 1 h. The products were analyzed by gas chromatograph (Shimadzu GC-17 A) equipped with a flame ionization detector. Product identification was also confirmed by GC-MS (Perkin Elmer Auto System XL Gas Chromatograph with Turbo Mass Spectrometer).

3. Results and discussion

3.1. Characterization of the catalysts

XRD provides direct information of pore architecture and phase purity of the materials. The XRD patterns of calcined samples with different n_{Si}/n_{Al} ratios are shown in Fig. 1. All calcined samples exhibit XRD patterns which is typical of a well ordered mesoporous materials and show an intense diffraction peak at low angle and at least three higher order peaks which can be indexed as (2 1 1), (2 2 0), (4 2 0) and (3 3 2) reflections. These features are consistent with a well-defined cubic structure, which is characteristic of Al-MCM-48. The XRD patterns are found to be in good agreement with previous reports for similar materials [26]. The position of reflections and the values of cubic unit cell constant of calcined Al-MCM-48 with different n_{Si}/n_{Al} ratios are given in

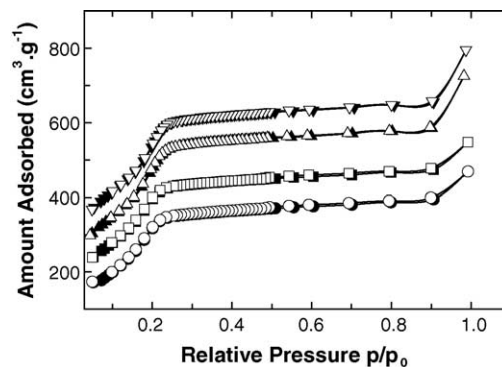


Fig. 2. Nitrogen adsorption isotherms (adsorption: closed symbols; desorption: open symbols) of Al-MCM-48 with different n_{Si}/n_{Al} ratio: (○) Al-MCM-48 (25); (□) Al-MCM-48 (50); (△) Al-MCM-48 (75); and (▽) Al-MCM-48 (100). The isotherms are shifted by 50 cm³/g upward for clarity.

Table 1. The d-spacings are compatible with cubic $Ia3d$ space group as reported in the literature [2]. The cubic unit cell constant a_0 was calculated according to $a_0 = d_{hkl} \sqrt{(h^2 + k^2 + l^2)}$. It is interesting to note that the unit cell parameter of the calcined Al-MCM-41-48 samples decreases with the decrease of n_{Si}/n_{Al} ratio, suggesting a decrease in wall thickness with increasing metal content (Table 1). The decrease in the unit cell constant is greater at higher Al content.

Adsorption technique is used to determine the porosity and specific surface area of materials. All calcined samples exhibit a typical reversible type IV adsorption isotherm as defined by IUPAC indicating the presence of mesopores. Fig. 2 shows the amount of nitrogen adsorbed versus relative pressure at 77 K for Al-MCM-48 of different n_{Si}/n_{Al} ratios. Three different well-defined stages are observed in the isotherms. At low relative pressure (p/p_0), adsorption occurs only as monolayer on the pore walls depicted by the initial increase in nitrogen uptake. As the relative pressure increases ($p/p_0 > 0.2$), a sharp inflection is observed characteristic of capillary condensation of nitrogen in mesopores. The sharpness of the inflection reflects uniformity of the pore sizes and the height indicates the pore volume. The linear part observed at higher p/p_0 is attributed to the multilayer adsorption on the external surface of the materials.

The BET surface area, pore volume, pore size and wall thickness of the calcined materials are presented in Table 1. The specific surface area calculated using BET model of all the samples are high demonstrating the mesoporous nature of the materials. The pore wall thickness is calculated using

Table 1
Physico-chemical characteristics of Al-MCM-48 catalysts

Catalyst	d_{211} spacing (nm)	a_0 (nm)	A_{BET} (m ² /g)	n_{Si}/n_{Al}		Pore volume (cm ³ /g)	Pore size (nm)	Wall thickness (nm)
				Gel	Product			
Al-MCM-48 (25)	3.06	7.50	1245	25	26	0.56	2.10	1.37
Al-MCM-48 (50)	3.13	7.67	1280	50	48	0.61	2.20	1.38
Al-MCM-48 (75)	3.19	7.81	1325	75	77	0.70	2.25	1.40
Al-MCM-48 (100)	3.22	7.89	1373	100	105	0.73	2.30	1.40

the formula: wall thickness = $a_0/3.0919 - \text{pore size}/2$ where 3.0919 is a constant representing the minimal surface area for MCM-48 space group [27,28]. From Table 1, it has been found that the specific surface area, specific pore volume, and the pore diameter of AlMCM-48 decrease with the increase of Al content. This could be mainly attributed to the presence of metal oxide species inside the mesoporous channels of AlMCM-48 with high Al content. A similar behavior has also been observed for metal substituted cubic and hexagonal type mesoporous materials [7,29]. In addition, the calculated pore wall thickness decreases with increasing Al content, which may be due to the reduced condensation of aluminosilicate polyanions as compared to the silicate polyanions. This reduces the degree of polymerization and lowers the pore wall thickness as well as the unit cell size of the product with the highest Al content.

The isomorphous substitution of silicon in the framework of MCM-48 by trivalent aluminium ions and its coordination can be directly evidenced by ^{27}Al MAS NMR spectra. The spectra of as-synthesized and calcined Al-MCM-48 catalysts with different $n_{\text{Si}}/n_{\text{Al}}$ ratios are shown in Fig. 3A and B, respectively. The spectra of as-synthesized samples exhibit a strong signal at ~ 53 ppm corresponding to the tetrahedral coordination of Al in the framework. The absence of a peak at 0 ppm for as-synthesized samples reveals the absence of octahedral Al coordination. In the case of calcined samples,

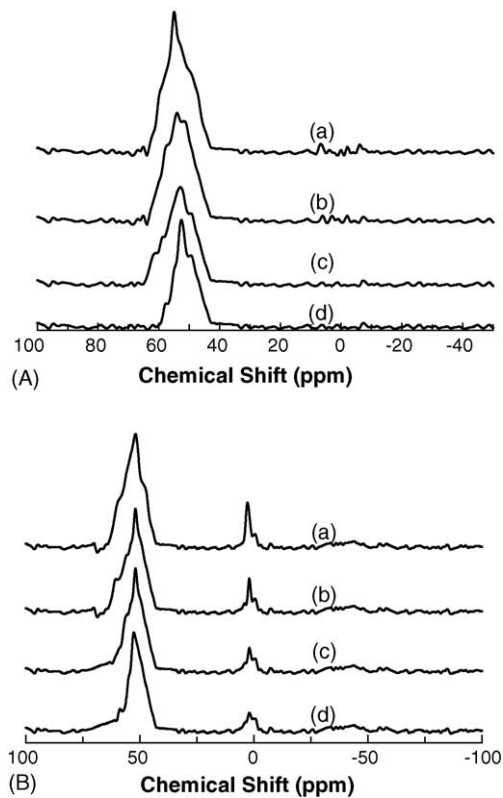


Fig. 3. ^{27}Al MAS NMR spectra of (A) as-synthesized and (B) calcined Al-MCM-48 catalysts with various $n_{\text{Si}}/n_{\text{Al}}$ ratios: (a) Al-MCM-48 (25); (b) Al-MCM-48 (50); (c) Al-MCM-48 (75); and (d) Al-MCM-48 (100).

a weak signal around 0 ppm shows the presence of Al in octahedral coordination, which indicates that during calcination some Al species are removed from the framework [30]. The intensity of these peaks increases as the Al content increases. The spectra of calcined samples also show a slight peak broadening of Al signals, which can be attributed to highly distorted environment [15,27].

The ^{29}Si MAS NMR spectra of as-synthesized and calcined samples of Al-MCM-48 (25) are shown in Fig. 1S (see supporting information). The spectrum of as-synthesized sample exhibits two main peaks at -109.6 and -100.8 ppm corresponding to $[\text{Si}(\text{OSi})_4]$ Q^4 units and $[\text{Si}(\text{OSi})_3(\text{OH})]$ Q^3 units respectively. A weak shoulder at -91.0 ppm corresponding to $[\text{Si}(\text{OSi})_2(\text{OH})_2]$ Q^2 units is also observed [31]. Calcination leads to decrease in peak intensity of Q^3 signals indicating the condensation of Si-OH groups, which can be correlated with the unit cell contraction observed in XRD. Similar results were observed by Huo et al. [32] in the formation of MCM-41 using XRD and ^{29}Si MAS NMR.

The pyridine adsorbed FT-IR spectrum is a useful tool for unambiguous determination of the nature of acid sites. Indeed, the spectra revealed the presence of both Lewis sites (bands at 1610 and 1445 cm^{-1}) and Brønsted sites (band at 1550 cm^{-1}) in all the catalysts (Fig. 4). The high intensity peak at 1550 cm^{-1} indicates that majority of acid sites present in the catalyst are of Brønsted type. The peak intensities of both Brønsted and Lewis acid sites are found to be high with increasing Al content. It is important that for acid catalyzed reactions, Brønsted acidity should be associated with the presence of tetrahedral Al and Lewis acidity is associated with octahedral Al [33]. Brønsted acidity is higher than Lewis acidity due to large number of tetrahedrally coordinated Al on the silica surface [12] in accordance with ^{27}Al MAS NMR.

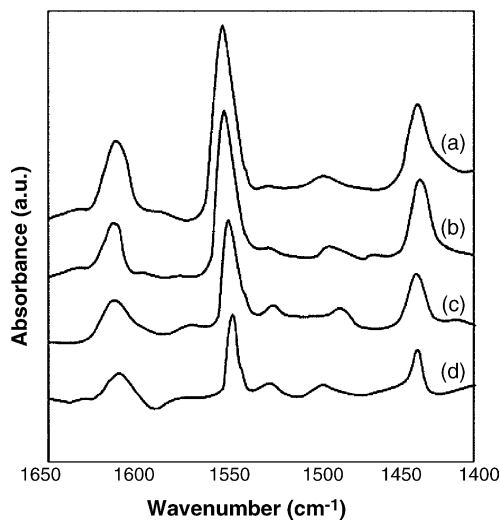


Fig. 4. Pyridine adsorbed FT-IR spectra of: (a) Al-MCM-48 (25); (b) Al-MCM-48 (50); (c) Al-MCM-48 (75); and (d) Al-MCM-48 (100) catalysts.

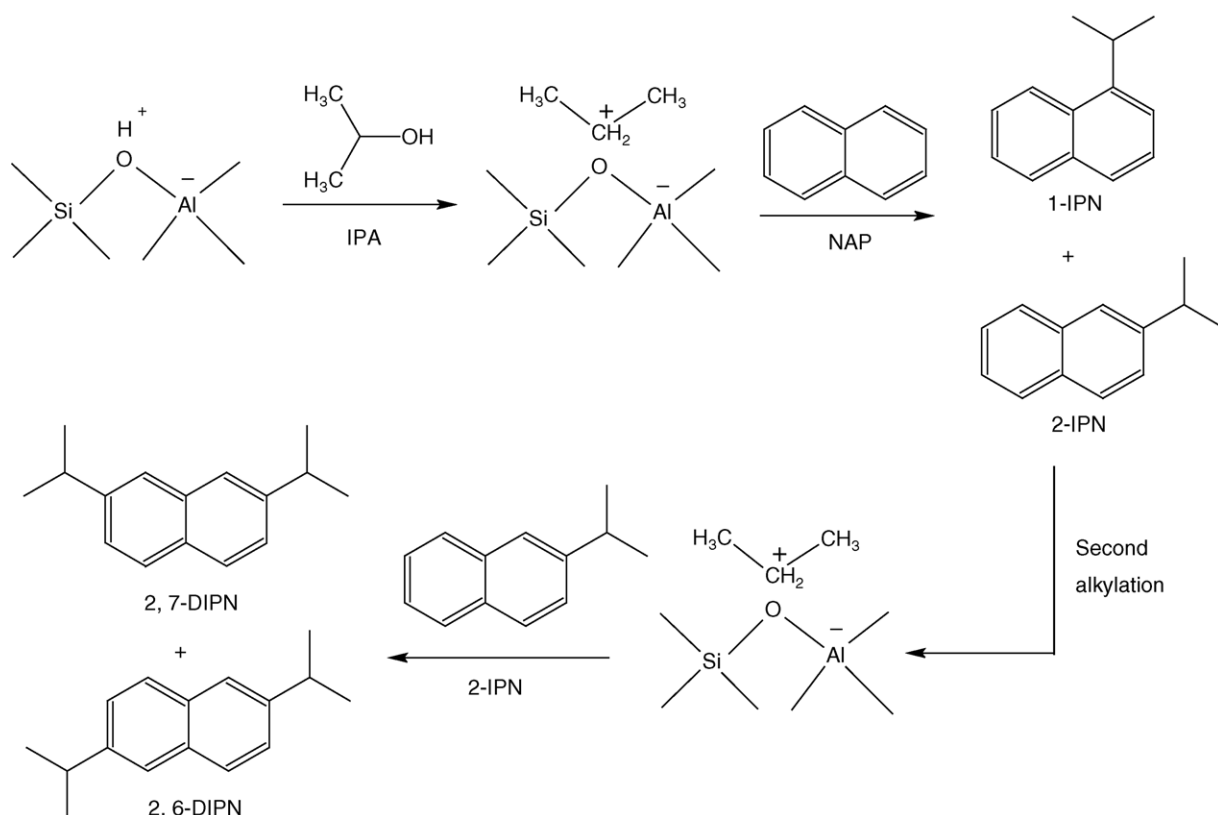
3.2. Catalytic studies

Isopropylation of NAP with IPA was carried out over Al-MCM-48 catalysts in the temperature range 250–400 °C in steps of 50 °C using cyclohexane as the solvent. The optimized molar ratio of 1:2:10 (NAP:IPA:CYH) was maintained and WHSV of 5.36 h⁻¹ was used for all the catalytic runs. In the alkylation reaction, formation of dialkylated product always accompanied mono-alkylated product. It is known that this reaction is a consecutive reaction [34]. The product analysis revealed the formation of mono-alkylated products like 1-isopropyl-naphthalene (1-IPN), 2-isopropyl-naphthalene (2-IPN) and dialkylated products like 2,6-diisopropyl-naphthalene (2,6-DIPN) and 2,7-diisopropyl-naphthalene (2,7-DIPN). As illustrated in Scheme 1, an isopropyl cation formed on the channel surface remained as charge-compensating cation which reacted with NAP in the vapour phase to yield the mono-alkylated products. The 2-IPN in turn reacts with one more isopropyl cation during its diffusion through the channel to yield 2,6-DIPN and 2,7-DIPN. The other diisopropyl-naphthalene isomers and polyisopropyl-naphthalene are included as PIPN in the tables. Analysis of the products also indicates that alkylation occurs preferentially at 2 and 6 positions of NAP. The slightly smaller critical diameter and more linear structure of 2,6-DIPN make it easier to diffuse in the pore channel. The detailed studies on the influence of various reaction param-

eters such as reaction temperature, WHSV, feed molar ratio and time on stream on NAP conversion and product selectivity particularly 2,6-DIPN in the isopropylation of NAP over Al-MCM-48 with different $n_{\text{Si}}/n_{\text{Al}}$ ratios using IPA as alkylating agent were carried out.

Isopropylation of NAP was carried out over the Al-MCM-48 catalysts with different $n_{\text{Si}}/n_{\text{Al}}$ ratios in the temperature range 250–400 °C in steps of 50 °C. The optimized molar ratio 1:2:10 (NAP:IPA:CYH) and WHSV (5.36 h⁻¹) were used for all catalytic runs. The NAP conversion over all the above catalytic systems at various reaction temperatures is given in Fig. 5 and products selectivity are presented in Table 2. NAP conversion is found to increase steadily with increasing reaction temperature up to 350 °C over all the catalytic systems. The Further increase in temperature resulted a significant decrease in conversion over all the catalytic systems. This could be mainly due to deactivation of the catalyst due to coking. A slight increase in selectivity of IPN is observed with a decrease in NAP conversion and selectivity of 2,6-DIPN and PIPN at 400 °C. This may be due to the secondary reactions like *trans*-alkylation and de-alkylation of DIPN. Based on the conversion of NAP and selectivity of 2,6-DIPN, 350 °C is considered to be the optimum reaction temperature.

Alkylation reactions are acid catalyzed requiring the presence of Brönsted acid sites generated by the framework trivalent Al atoms. The catalytic activity of the mesoporous



Scheme 1. Proposed reaction scheme for alkylation of naphthalene with isopropyl alcohol over Al-MCM-48 catalyst.

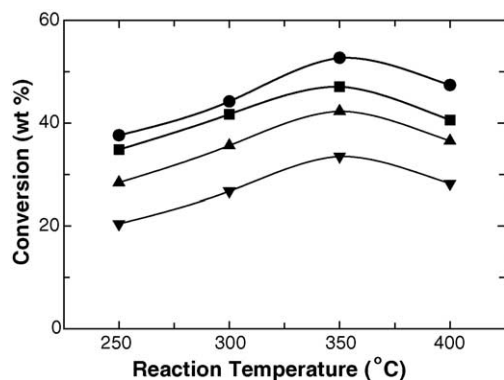


Fig. 5. Effect of temperature on naphthalene conversion over Al-MCM-48 catalysts with various $n_{\text{Si}}/n_{\text{Al}}$ ratios. Reaction conditions: feed molar ratio = 1:2:10 (NAP:IPA:CYH); WHSV = 5.36 h^{-1} ; weight of catalyst = 0.5 g; time on stream = 1 h: (●) Al-MCM-48 (25); (■) Al-MCM-48 (50); (▲) Al-MCM-48 (75); and (▼) Al-MCM-48 (100).

materials reflects changes in the location of the Al sites and acidic strength (or acid site density) depending on the Al content. From Fig. 5, it is observed that increase in Al content as well as total acidity increase the NAP conversion at all the temperatures studied. Al-MCM-48 (25) shows maximum conversion of 52.7 wt.% at 350 °C. The observed increase in NAP conversion with increasing incorporation of Al content may be due to the additional increase in Brönsted acidity leading to high density of acid sites generated by Al incorporation as evidenced by acidity measurements.

The influence of $n_{\text{Si}}/n_{\text{Al}}$ ratio of the samples on the product selectivity in the isopropylation of NAP at 350 °C is also given in Table 2. It is observed that 2,6-DIPN selectivity increases with increase in Al content and in contrast the mono-alkylated products decrease. The catalyst has low Al content in higher $n_{\text{Si}}/n_{\text{Al}}$ ratio, which is not sufficient for di-alkylation. Thus decrease in formation of di-alkylated products at higher $n_{\text{Si}}/n_{\text{Al}}$ ratio catalysts is due to the inaccessibility of the active sites for the reactant molecules as many Al sites are found inside the pores. The mono-alkylated products are found to be higher at high $n_{\text{Si}}/n_{\text{Al}}$ ratio as number of acid sites is less and less possibility of IPN to undergo further alkylation. The reusability of the catalyst was tested and it was found that the catalytic activity was retained. This was further confirmed by XRD. The XRD patterns of the reused

catalyst show similar intensity of planes as that of fresh catalyst (not shown).

Among the dialkylated NAP, the selectivity for 2,6-DIPN was always higher than 2,7-DIPN. This is also reflected in the ratio of 2,6-/2,7-DIPN shown in Table 2. Song et al. [35] put forward the restricted electronic transition-state selectivity based on frontier electron density, which reveals that the carbon at position 6 of 2-IPN has higher frontier electron density than that of position 7. According to the frontier molecular orbital theory, the most reactive position has the highest frontier electron density. Thus the formation of 2,6-DIPN is more electronically favored than that of 2,7-DIPN. In the present study the formation of 2,6-DIPN is higher than 2,7-DIPN for all the catalysts with different $n_{\text{Si}}/n_{\text{Al}}$ ratios. The higher selectivity towards 2,6-DIPN is due to low energy barrier for the diffusion of 2,6-DIPN (4 kcal/mol) that is significantly less than 2,7-DIPN (18 kcal/mol) based on the computer simulation calculation studies by Horsley et al. [36]. The decrease of 2,6/2,7-DIPN ratio with increase in $n_{\text{Si}}/n_{\text{Al}}$ ratio is due to decrease in acidity, which reduces the isomerisation. Strong acidity is capable of isomerising the alkylaromatics and hence the more strained 2,7-DIPN is isomerised to less strained 2,6-DIPN. This can be further confirmed by trend in the change of temperature where the selectivity towards 2,6-DIPN increases with increase in temperature. The energy barrier for 2,7-DIPN is higher than 2,6-DIPN. Thus, higher energy is required for the isomerisation of 2,7-DIPN to 2,6-DIPN which enhances with increase in temperature. Therefore, it can be concluded that 2,6-DIPN selectivity not only depends on the acid site density but also on the diffusional properties and experimental conditions.

Isopropylation of NAP with IPA was carried out at 350 °C over Al-MCM-48 (25) with varying NAP to IPA molar ratios (1:1, 1:2, 1:3 and 1:4) by keeping the molar ratio of solvent to NAP as 10. Naphthalene conversion and products selectivity at various molar feed ratios are presented in Table 3. It is found that both activity and selectivity are influenced drastically by change of reactant ratio. The conversion of NAP and PIPN selectivity rapidly increase with the increase of IPA in the reactant mixture. It can be accounted that polar molecule such as IPA competes with NAP for adsorption sites and with increasing molar excess of alkylating agent, the NAP conversion increases which is in line with other reports [37]. The

Table 2
Products distribution of isopropylation of naphthalene over different catalysts at different reaction temperatures

Catalysts	Temperature (°C)	Conversion (%)	Product selectivity (%)					2,6/2,7-DIPN
			1-IPN	2-IPN	2,6-DIPN	2,7-DIPN	PIPN	
Al-MCM-48 (25)	250	37.6	11.2	32.1	42.7	6.1	7.9	7.0
	300	44.2	10.3	29.6	45.1	6.3	8.7	7.1
	350	52.7	9.2	24.1	48.7	6.5	11.5	7.5
	400	47.4	8.3	22.5	49.8	6.8	12.6	7.3
Al-MCM-48 (50)	350	47.1	12.6	31.2	39.8	5.9	10.5	6.7
Al-MCM-48 (75)	350	42.3	14.2	36.7	33.8	5.8	9.5	5.8
Al-MCM-48 (100)	350	33.5	16.2	41.3	28.1	5.6	8.8	5.0

Reaction conditions: feed molar ratio = 1:2:10 (NAP:IPA:CYH); WHSV = 5.36 h^{-1} ; weight of catalyst = 0.5 g; time on stream = 1 h.

Table 3
Effect of feed molar ratio on the products selectivity over Al-MCM-48 (25)

Feed ratio (NAP:IPA)	Conversion (wt.%)	Product selectivity (wt.%)				
		1-IPN	2-IPN	2,6-DIPN	2,7-DIPN	PIPn
1:1	45.2	12.6	27.8	45.7	6.7	7.2
1:2	52.7	9.2	24.1	48.7	6.5	11.5
1:3	55.4	7.7	22.2	47.6	5.8	16.7
1:4	56.5	6.5	19.7	43.7	5.0	25.3

Reaction conditions: weight of catalyst = 0.5 g; time on stream = 1 h; WHSV = 5.36 h⁻¹; temperature = 350 °C.

Table 4
Effect of WHSV on product selectivity over Al-MCM-48 (25)

WHSV (h ⁻¹)	Conversion (wt.%)	Product selectivity (wt.%)				
		1-IPN	2-IPN	2,6-DIPN	2,7-DIPN	PIPn
4.50	53.6	8.9	23.6	47.5	6.3	13.7
5.36	52.7	9.2	24.1	48.7	6.5	11.5
6.54	49.5	11.7	26.7	45.3	7.4	8.9
8.75	40.3	14.1	28.8	42.2	8.5	6.4

Reaction conditions: weight of catalyst = 0.5 g; time on stream = 1 h; feed molar ratio = 1:2:10 (NAP:IPA:CYH); temperature = 350 °C.

β,β' -selectivity is found to increase with increase in IPA in the feed upto 1:2 (NAP:IPA) and a decrease in trend is observed with further increase in IPA. This can be explained by the consecutive alkylation of IPN by IPA into DIPN and then into PIPN. This is facilitated by the high concentration of IPA in the reaction mixture which can provide higher availability of isopropyl cations. Based on the NAP conversion and 2,6-DIPN selectivity, the optimum molar ratio of 1:2 (NAP:IPA) is taken for further studies.

The influence of WHSV on alkylation of NAP with IPA over Al-MCM-48 (25) at 350 °C is shown in Table 4. The molar ratio of the feed was maintained at 1:2:10 (NAP:IPA:CYH). A slight decrease in NAP conversion was observed when the WHSV was increased from 4.5 to 5.36 h⁻¹. Further increase in WHSV drastically decreased the NAP conversion. The reduction in conversion may be simply due to high diffusion of the reactant molecules owing to shorter contact time at higher space velocity. The catalytic activity decreased very slowly at low WHSV whereas the decreasing rate quickened at high WHSV. Since the alkylation reaction is consecutive, when WHSV is high only a small part of IPN has enough reaction time to be further alkylated into DIPN and PIPN subsequently indicating the high selectivity for IPN at high WHSV. Hence it is reasonable to choose low WHSV for good conversion and selectivity of DIPN. The selectivity of 2,6-DIPN and PIPN has been found to decrease with increasing WHSV above 5.36 h⁻¹, which may be due to trans-alkylation of DIPN and PIPN to IPN and NAP.

The sustainability of the catalysts in the isopropylation of NAP was studied by carrying out the time on stream studies for a duration of 6 h at 350 °C. An optimized feed ratio of 1:2:10 (NAP:IPA:CYH) and WHSV (5.36 h⁻¹) were maintained during the time on stream studies. The products were collected at a time interval of every 1 h. Coke deposition over the catalyst surface during the reaction is a crucial factor leading to the deactivation of a catalyst [38]. The deactivation of

faujasite during isopropylation of benzene is due to blocking (poisoning) of active sites while deactivation of mordenite is due to blocking of the channels by bulkier molecules like DIPB [39]. Coke formation and diffusion problems can be prevented by using three dimensional mesoporous catalysts. The NAP conversion over different catalysts during the time on stream study is presented in Fig. 2S (see supplementary information). The decrease in the conversion of NAP is marginal after several hours of time which indicates that Al-MCM-48 does not deactivate quickly. This may be due to its three-dimensional pore structure which limits pore blocking and allows faster diffusion of reactant molecules than one-dimensional pore system such as Al-MCM-41 [7,30,40]. Moreover alcohols reduce deactivation as the formation of olefins from cracking is difficult which block the active sites and makes it inaccessible for the reactant molecules. Alcohols are less prone to cracking than the acetates [41] and diethyl carbonates [42] which are used as alkylating agents.

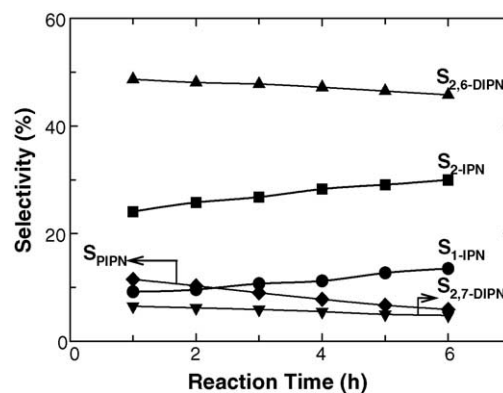


Fig. 6. Effect of time on stream on the product selectivity over Al-MCM-48 (25) catalyst at 350 °C. Reaction conditions: weight of catalyst = 0.5 g; WHSV = 5.36 h⁻¹; feed molar ratio = 1:2:10 (NAP:IPA:CYH); (●) S_{1-IPN}; (■) S_{2-IPN}; (▲) S_{2,6-DIPN}; (▼) S_{2,7-DIPN}; and (◆) S_{PIPn}.

The product selectivity over Al-MCM-48 (25) during time on stream is presented in Fig. 6. It is found that there is no appreciable change in selectivity of the products.

4. Conclusion

The structural and textural properties of the synthesized materials have been characterized by employing various physicochemical techniques. Moderate Brønsted acidity generated by the isomorphic substitution of Si by Al during the synthesis, gives rise to a substantial catalytic activity tested by isopropylation of NAP by IPA. Both NAP conversion and selectivity can be altered by adjusting the reaction parameters such as temperature, space velocity and feed ratio. High temperature, moderate acidity and longer contact time help to improve NAP conversion and 2,6-DIPN selectivity. Among the catalysts used in the present study, AlMCM-48 (25) showed a high NAP conversion and selectivity to 2,6-DIPN under the optimized reaction conditions. It has been found that the selectivity for 2,6-DIPN was always higher than 2,7-DIPN for all the catalysts. The three dimensional pore system of AlMCM-48 easily allows easy diffusion of 2,6-DIPN which has very low energy barrier for diffusion as compared to 2,7-DIPN. It has also been found that the three dimensional AlMCM-48 catalyst is very stable and reusable. The conversion of NAP over AlMCM-48 was maintained when the reaction was carried out for several hours of reaction time.

Acknowledgments

A. Vinu is grateful to Prof. Y. Bando and Special Coordination Funds for Promoting Science and Technology from the Ministry of Education, Culture, Sports, Science and Technology of the Japanese Government for the award of ICYS Research Fellowship, Japan. One of the authors, V. Murugesan, expresses his sincere thanks to generous financial support of the Department of Science and Technology (Sanction No. SR/S1/PC-24/2003), Government of India, New Delhi. T. Krithiga thanks CSIR, India for Senior Research Fellowship.

Appendix A. Supplementary data

Supplementary data associated with this article can be found, in the online version, at [doi:10.1016/j.molcata.2005.05.008](https://doi.org/10.1016/j.molcata.2005.05.008).

References

- [1] C.T. Kresge, M.E. Leonowicz, W.J. Roth, J.C. Vartuli, J.S. Beck, *Nature* 359 (1992) 710.
- [2] J.S. Beck, J.C. Vartuli, W.J. Roth, M.E. Leonowicz, K.D. Schmidt, C.T.W. Chu, D.H. Olson, E.W. Sheppard, S.B. McCullen, J.B. Higgins, J.L. Schlenker, *J. Am. Chem. Soc.* 114 (1992) 10834.
- [3] J.C. Vartuli, K.D. Schmidt, C.T. Kresge, W.J. Roth, M.E. Leonowicz, S.B. McCullen, S.D. Hellring, J.S. Beck, J.L. Schlenker, D.H. Olson, E.W. Sheppard, *Chem. Mater.* 6 (1994) 2317.
- [4] Q. Huo, D.I. Margolese, G.D. Stucky, *Chem. Mater.* 8 (1996) 1147.
- [5] J. Xu, Z. Luan, M. Hartmann, L. Kevan, *Chem. Mater.* 11 (1999) 2928.
- [6] K. Schumacher, M. Grun, K.K. Unger, *Microporous Mesoporous Mater.* 27 (1999) 201.
- [7] H. Kosslick, G. Lischke, H. Landmesser, B. Partitz, W. Storek, R. Fricke, *J. Catal.* 176 (1998) 102.
- [8] A. Vinu, V. Murugesan, W. Böhlmann, M. Hartmann, *J. Phys. Chem. B* 108 (2004) 11496.
- [9] A. Vinu, M. Hartmann, *Chem. Lett.* 33 (2004) 588.
- [10] A. Vinu, K. Usha Nandhini, V. Murugesan, W. Böhlmann, V. Umamaheswari, A. Pöppel, M. Hartmann, *Appl. Catal. A: Gen.* 265 (2004) 1.
- [11] A. Vinu, T. Krithiga, V. Murugesan, M. Hartmann, *Adv. Mater.* 16 (2004) 1817.
- [12] A. Corma, *Chem. Rev.* 97 (1997) 2373.
- [13] H. Kosslick, G. Lischke, G. Walther, W. Storek, A. Martin, R. Fricke, *Microporous Mater.* 9 (1997) 13.
- [14] A. Sakthivel, S.K. Badamali, P. Selvam, *Microporous Mesoporous Mater.* 39 (2000) 459.
- [15] K. Chaudhari, T.K. Das, A.J. Chandwadkar, S. Sivasanker, *J. Catal.* 186 (1999) 81.
- [16] J.R. Trotter, B.J. Sublett, U.S. Patent 5,013,820 (1991).
- [17] R. Brzozowski, W. Skupinski, *J. Catal.* 210 (2002) 313.
- [18] A.D. Schmitz, C. Song, *Catal. Lett.* 40 (1996) 59.
- [19] R. Maheswari, K. Shanthi, T. Sivakumar, S. Narayanan, *Appl. Catal. A* 6479 (2003) 1.
- [20] A. Katayama, M. Toba, G. Takeuchi, F. Mizukami, S. Niwa, S. Mitamura, *J. Chem. Soc., Chem. Commun.* (1991) 39.
- [21] R. Anand, R. Maheswari, K.U. Gore, S.S. Khaire, V.R. Chumbhale, *Appl. Catal. A* 249 (2003) 265.
- [22] J. Wang, J.N. Park, Y.K. Park, C.W. Lee, *J. Catal.* 220 (2003) 265.
- [23] G. Kamalakar, S.J. Kulkarni, K.V. Raghavan, S. Unnikrishnan, A.B. Halgeri, *J. Mol. Catal. A* 149 (1999) 283.
- [24] C. Subrahmanyam, B. Viswanathan, T.K. Varadarajan, *J. Mol. Catal. A* 226 (2005) 155.
- [25] X.S. Zhao, G.Q. Lu, C. Song, *Chem. Commun.* (2001) 2306.
- [26] Y. Xia, R. Mokaya, *J. Phys. Chem. B* 107 (2003) 6954.
- [27] M. Hartmann, C. Bischof, *J. Phys. Chem. B* 103 (1999) 6230.
- [28] K. Schumacher, P.I. ravikovitch, A.D. Chesne, A.V. Neimark, K.K. Unger, *Langmuir* 16 (2000) 4648.
- [29] M. Kruk, M. Jaroniec, A. Sayari, *Langmuir* 15 (1999) 5683.
- [30] S.E. Dapurkar, P. Selvam, *Appl. Catal. A* 254 (2003) 239.
- [31] C.Y. Chen, H.X. Li, M.E. Davis, *Microporous Mater.* 2 (1993) 17.
- [32] Q. Huo, D.I. Margolese, U. Ciesla, *Chem. Mater.* 6 (1994) 1176.
- [33] H.D. Lanh, V.A. Tuan, H. Kosslick, B. Parltitz, R. Fricke, *J. Volfer, Appl. Catal. A* 103 (1993) 205.
- [34] G. Colon, I. Ferino, E. Rombi, E. Selli, L. Forni, P. Magnoux, M. Guisnet, *Appl. Catal. A* 168 (1998) 81.
- [35] C. Song, X. Ma, A.D. Schmitz, H.H. Schobert, *Appl. Catal. A* 182 (1999) 175.
- [36] J.A. Horsley, J.D. Fellmann, E.G. Derouane, C.M. Freeman, *J. Catal.* 147 (1994) 231.
- [37] R.F. Parton, J.M. Jacobs, D.R. Huybrechts, P.A. Jacobs, *Stud. Surf. Sci. Catal.* 46 (1989) 163.
- [38] C. Flego, G. Pazzuconi, E. Beneini, C. Perego, *Stud. Surf. Sci. Catal.* 126 (1999) 461.
- [39] A.R. Pradhan, B.S. Rao, *J. Catal.* 132 (1991) 79.
- [40] S.B. Pu, J.B. Kim, M. Seno, M.T. Inui, *Microporous Mater.* 10 (1997) 25.
- [41] S. Udayakumar, A. Pandurangan, P.K. Sinha, *J. Mol. Catal. A: Chem.* 216 (2004) 75.
- [42] S. Udayakumar, A. Pandurangan, P.K. Sinha, *Appl. Catal. A* 272 (2004) 267.